International Journal of Heat and Technology
Vol. 36, No. 4, December, 2018, pp. 1443-1449
Journal homepage: http://iieta.org/Journals/IJHT

Effect of jet width and momentum coefficient of active control over NACA0012 airfoil using synthetic jet

Mohamed C. Saadi*, Lakhdar Bahi

Department of Physic, Laboratory of Physic Energetic, Fréres Mentouri Constantine1 University, Constantine, Algeria

Corresponding Author Email: saadi_med_cherif@yahoo.com

https://doi.org/10.18280/ijht.360437

Received: 18 January 2018
Accepted: 13 September 2018

Keywords:
control, flow separation, synthetic jet, NACA0012 profile

ABSTRACT

In this study, the effect of the jet control width and its momentum coefficient on the flow over a NACA0012 airfoil is investigated numerically for a Reynolds number equal to $2.88x10^6$. The jet is placed at 15% of the chord length from the leading edge on the upper surface of the airfoil. The calculation was carried out using the solver URANS with the (k-ε) RNG model. Simulation results for an incompressible fully turbulent flow, varying the jet width from 0.5 to 3.5 percent of the chord length with jet control angle β equal to 45^0, the lift to drag ratio increase. However, an optimum jet width of 2% of the profile chord, leads to better performance. I is also be observed, when the momentum coefficient rises, the lift coefficient increases reaching about 86% improvement (for better improvement by 85.93%) and the stall angle is delayed from 16^0 to 22^0. This parametric study led to select the control parameters for the best aerodynamic performance of the airfoil.

1. INTRODUCTION

In recent years, the control of the boundary layer separation used in most aerodynamic applications, whether internal or external flows, is an important topic which is widely discussed by the scientific community. In fact, the development of control techniques leads to improve aerodynamic performance, reduce consumption, fuel and minimize pollution and noise. The control approaches take advantages of the natural instability of shear layer separated [1]. Many control techniques have been developed, which may be classified into two categories, passive and active flow controls [2]. The passive control flow, requiring no external energy input, but their impact on the reduction of drag remains low [3.4]. Examples of passive means are slats, flaps and vortex generators [5-6]. In contrast, using active flow control technique, involves an external energy to modify lift and drag on an airfoil. Several active flow control is tested to find out its efficiency and reliability. The use periodic blowing and suction [7-8], acoustic and thermal methods [9-10], or electromagnetic [11]. In the most publications, synthetic jet actuators are used as an active flow control technique. Tuck and Soria [12] conducted an experimental study over NACA0015 using synthetic jet. Measurements indicated when a non-dimensional frequency is 1.3 and the excitation momentum coefficient is 0.14%, the lift coefficient increases. Zaman et al. [13] installed a loudspeaker outside an LRN (1)-1007 airfoil. The acoustic excitation from loudspeaker suppressed flow separation. The Result showed that the lift coefficient increased by 50% at $\alpha \geq 18$deg. Hui Tang et al. [14] studied the aerodynamic performance using synthetic jet arrays. The experimental results showed that the jet can delay boundary layer separation which increases the lift coefficient by 27% and reduces the drag coefficient about 19%. Another work is presented by McCormick [15] showed that a tangential synthetic jet can improve the aerodynamic performance of profile taking into account an oscillation frequency (F^+=1, 3) and jet momentum coefficient (Cμ=0.5%), the synthetic jet actuator placed at 4% chord from the leading edge. Results indicated that the stall angle is pushed from about 6^0 and the maximum lift coefficient increased by 25%.

Several numerical [16-18] studies showed that using flow separation control, such as suction, blowing and synthetic (zero-net-mass-flux) jet, causes the larger lift coefficient for different NACA airfoils. Rosas [19] studies on flow separation control on a NACA0012 airfoil using synthetic jets. The numerical results indicated that the lift coefficient increased by 93%. Esmaeili et al. [20] showed that a tangential synthetic jet over NACA23012 profile, with a dimensionless frequency jet (F^+= 0,159 and F^+=1) and blowing ratio (Vj/U∞) between 0 to 5 synthetic jet slope of an angle (αj), included between (0^0 to 83^0). It is concluded that an increasing blowing ratio resulted in increasing lift to drag ratio. Donovan et al. [21] investigated flow reattachment over a NACA0012 airfoil using time-harmonic zero mass flux blowing. Those results indicated a 20% post-stall increase in lift at $\alpha=22^0$. Piperas as in 2010 studied in flow separation control on an NACA4415 airfoil through different suction when the maximum lift coefficient increased by 20 percent [22]. Flow separation control by SJ on NACA0015 profile using LES method is studied by D. You et al. [23]. This study shows that when the parameters of control are analyzed, the lift and drag coefficients are enhanced by 70 percent and 18 percent, respectively. Akcayoz et al. [24] studied the optimum parameters of synthetic jet over NACA0012 profile with different angles of attack. The results indicated that optimum performance is marked when the jet location moved toward leading edge and an optimum jet angle increased as the angle of attack increased. E. Montazer et al. [25] applied a synthetic jet on a NACA0015 profile at the stall and post stall angles of attack $\alpha=13^0$ and 16^0 respectively. The results of numerical simulation indicated a significant effect on the post stall angles

of attack, where the lift to drag ratio increased by 66%. Flow separation control by SJ over NACA0015 airfoil using Spalat-Allmaras (S-A) turbulence model is studied by M.A.boukenkoul et al. [26]. This study shows that when the parameters of control are analyzed, the stall angle delayed from 15^0 to 19^0 with enhancing the lift coefficient by 40%. K.N.Abedet et al. [27] investigated the effect synthetic jet for two positions placed at 3% and 6% of the chord length upper surface of a NACA0015 airfoil in Reynolds number Re = $4.4x10^5$, the experimental results showed a maximum enhancement in lift of about 0.2 at 6% chord length from leading edge SJA location.

In this paper, the study is aimed at expanding the database of synthetic jet applications in flow field control and identifying the main limitations for obtaining a control effective using jet width, jet momentum and jet angle parameters. Two-dimensional simulation over NACA0012 profile is adopted for active control with synthetic jet. The results with and without control show significant improvements in aerodynamic performances. Therefore, an optimum jet width and again in lift and with a positive shift in the value of the stall angle, is obtained.

2. NUMERICAL SIMULATION

2.1 Governing equations

The flow around the airfoil is simulated using the unsteady, Reynolds-averaged Navier-Stokes (URANS) equations, which in the incompressible form can write as follows

$$\frac{\partial \rho}{\partial t} + \frac{\partial (\rho u)}{\partial x} + \frac{\partial (\rho v)}{\partial y} = 0 \tag{1}$$

$$\rho\left(\frac{\partial u}{\partial t} + u\frac{\partial u}{\partial x} + v\frac{\partial u}{\partial y}\right) = -\frac{\partial p}{\partial x} + \mu\left(\frac{\partial^2 u}{\partial x^2} + \frac{\partial^2 u}{\partial y^2}\right) + \rho g_x \tag{2}$$

$$\rho\left(\frac{\partial v}{\partial t} + u\frac{\partial v}{\partial x} + u\frac{\partial v}{\partial y}\right) = -\frac{\partial p}{\partial y} + \mu\left(\frac{\partial^2 v}{\partial x^2} + \frac{\partial^2 v}{\partial y^2}\right) + \rho g_y \tag{3}$$

The model k-$^{\varepsilon}$ RNG was used to solve turbulence equations. This model is used in the present computation for its relatively accurate and economic benefit in term of time. The transport equations can written as follows:

Equation de transport turbulent kinetic energy k-$^{\varepsilon}$ RNG

$$\frac{\partial(\rho k)}{\partial t} + \frac{\partial(\rho k u_i)}{\partial x_i} = \frac{\partial}{\partial x_j}\left[\left(\alpha_k \mu_{eff}\right)\frac{\partial k}{\partial x_j}\right] + G_K + G_b - \rho\varepsilon - Y_M + S_k \tag{4}$$

Equation de transport du taux de dissipation ε l'énergie cinétique turbulent:

$$\frac{\partial(\rho\varepsilon)}{\partial t} + \frac{\partial(\rho\varepsilon u_i)}{\partial x_i} = \frac{\partial}{\partial x_j}\left(\alpha_\varepsilon \mu_{eff}\frac{\partial \varepsilon}{\partial x_j}\right) + C_{1k}\frac{\varepsilon}{k}\left(G_k + C_{3\varepsilon}G_b\right) - C_{2\varepsilon}\rho\frac{\varepsilon^2}{k} - R_\varepsilon + S_\varepsilon \tag{5}$$

In these equations, G_k represents the generation of turbulence kinetic energy due to the mean velocity gradients, G_b is the generation of turbulence kinetic energy due to buoyancy, Y_M represents the contribution of fluctuation dilatation in compressible turbulence to the overall dissipation rate. The quantities α_k and α_ε are the inverse effective Prandtl numbers for k and ε, respectively. S_k and S_ε are user-defined source terms. $C_{1\varepsilon}$, $C_{2\varepsilon}$, $C_{3\varepsilon}$ are constant.

2.2 Computation procedures

The commercial code " Fluent " solver is used as a CFD-tool for solving the governing equation. The flow model considered in the present study is based on 2D configuration, unsteady, incompressible regime and fully turbulent. The finite volume is used to discretize the unsteady RANS equations for turbulent flows to be solved. The terms of the convection velocity field and turbulent quantities are discretized by a scheme "UPWIND" second order. Pressure-velocity coupling is achieved using the "SIMPLE" method. The time advancement is determined by the fixed time step 0.002 second steps for both controlled case F^+=1.25 (f=50HZ) [28] with 100 time-steps in one oscillation period. Concerning the boundary condition, the velocity-inlet components and turbulent parameters are imposed at the periphery contour and outflow is use outlet and no-slip wall boundary conditions are defined for surfaces of the airfoil. Concerning the slot jet of control a user defined function (UDF) is developed to represent an oscillate diaphragm (SJ) (fig.1) [29-31]. The synthetic jet is defined as the following time function

$$U_j = U_0 \operatorname{Sin}\left(2\pi\frac{F^+ U}{c}t\right) \tag{6}$$

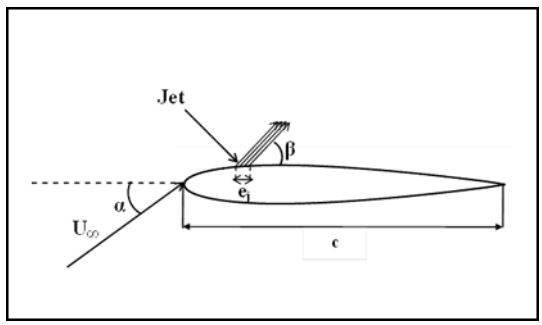

Figure 1. Profile geometry with jet

The parameters of the jet that affect the external fluid are [32]:

The non-dimensional frequency of a synthetic jet is defined as:

$$F^+ = \frac{fc}{U} \tag{7}$$

The coefficient of the jet momentum of the non-dimensional is:

$$C_\mu = \frac{\rho_j e_j U_0^2}{\frac{1}{2}\rho U^2} \tag{8}$$

The ratio between the jet velocity and upstream velocity is:

$$V_r = \frac{U_0}{U} \tag{9}$$

2.3 Grid generation

In this study, NACA0012 airfoil used for simulation. The Reynolds number and Mach number selected for clean profile validation and application of synthetic jet are Re=2.88x10^6 and M=0.13 (U=40m/s) respectively with a chord length of the airfoil c=1m [33].

The C-H type structure grid is generated over the clean airfoil, which is shown in (fig.2 (a)). The computational area was large enough to prevent the outer limit from affecting the near flow field around the airfoil. whereas others grid generated when jets placed at 15% chord from the leading edge for the different jet slot width 0.5%, 1%, 1.5%, 2%, 2.5%, 3%, 3.5% of chord length (fig.2 (b)) [34]. The mesh with and without control is generated using a commercial software "Gambit" pre-processing along with the boundary conditions. Various meshes were created with the aim of minimizing the number of cells to avoid long calculations and getting consistent results on the one hand and assure the mesh dependence in the other hand the mesh retained contains almost 52000 cells. For good prediction of the turbulent flow, a C-H type grid is used with mesh Refinement near a profile surface quantifying strong gradients.

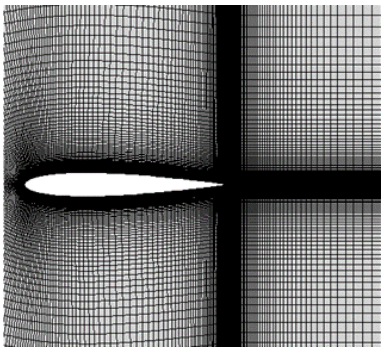

(a)

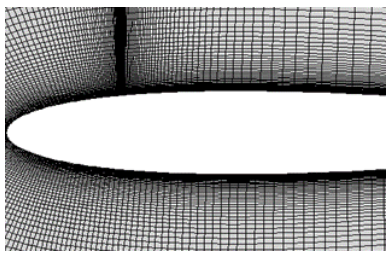

(b)

Figure 2. Computational grids used for the clean airfoil (uncontrolled airfoil) validation (a) and for controlled study (b)

3. VALIDATING RESULTS

Computational model is tested for a configuration of an uncontrolled NACA0012 airfoil with an angle of attack equal to15^0 where the separation flow appears. Comparison of the pressure coefficient distribution between the numerical and experimental results given by N.Gregory et al. [33] is illustrated in Fig. 3

The figure shows, the curves coincide at the upper surface (extrados) except at the leading edge where the pressure coefficient for the experimental case is higher. The difference is that in the experimental case we have the transition phenomenon as the boundary layer starts first laminar and becomes turbulent after that, while in the present numerical study the boundary layer is supposed fully turbulent along the whole surface airfoil. However, the overall results show a good concordance between the two cases at the upper surface where the separation takes place and where the control concept will be applied.

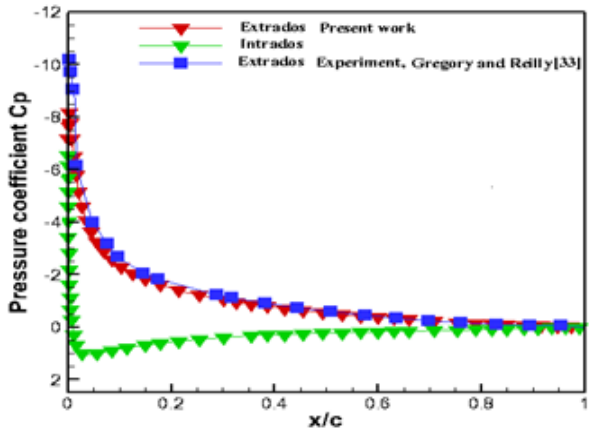

Figure 3. Comparison between experimental and numerical results for NACA0012 profile upper-surface pressure distributions without control (α=15^0, M=0.13 and Re=2.88x10^6)

4. RESULTS AND DISCUSSION

4.1 Effect of jet width on the separation control

Figures (4-6), present the lift, drag, and lift to drag ratio for different jet width with relative velocity Vr= 1.5 and jet slope angle β=45^0 at jet location 15% of chord length from the leading edge, respectively. The aerodynamic coefficients increase continuously as the jet width increase. When the jet width varied from 0.5% to 3% of the chord length, the lift coefficient increased by 25.62%, 30.76% and 48%, respectively, for the angles of attack of the 18^0, 20^0, 22^0, indicated an improvement in lift. Whereas in these cases drag is almost increased approximately linearly, resulting in no improvement in drag. Where, the jet promotes the mixing of the boundary layer and thus increase the amount of movement added thereto, which effectively delays the separation phenomenon. While keeping the boundary layer more turbulent for the higher angles of attack, when jet width increased. The lift to drag ratio increases until the jet width 2% of the chord length by 3.20%, 10.38%, and 16.40% for the angle of attack of the 18^0, 20^0, 22^0. Then decreases up to jet widths 3% of the chord length, indicating an optimum value in 2% of the chord length.

The following figure 7 indicate the averaged flow fields in one period for angle of attack α=20^0, the detail of the flow field is illustrated by streamline pattern for different jet width values 0.5%, 1%, 1.5%, 2%, 2.5% and 3% of the chord length. One can see that the separation zone is markedly reduced

respectively, resulting an improvement in performance aerodynamic. In fig.8, the location of the separation point for the different controlled configuration is quantified, to illustrate that the separation point is shifted until to 78% of chord near the trailing edge when the jet width is 3% of the chord length.

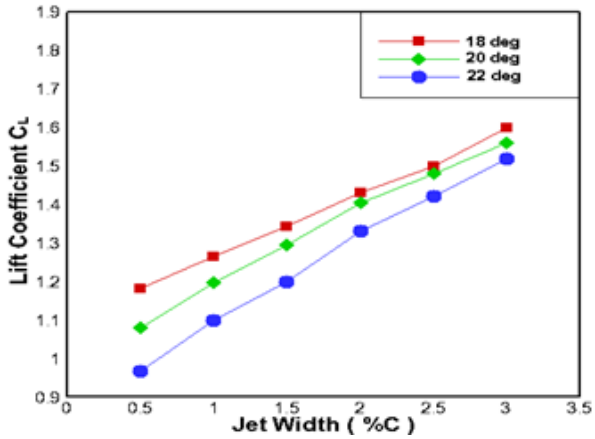

Figure 4. Evolution of lift coefficient on NACA0012 profile, M=0.13 for different values of jet width and angle of attack $\alpha = 18^0, 20^0, 22^0$

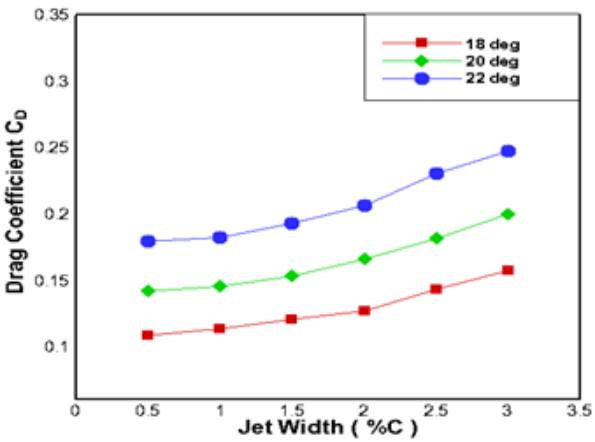

Figure 5. Evolution of drag coefficient on NACA0012 profile, M=0.13 for different values of jet width and angle of attack $\alpha = 18^0, 20^0, 22^0$

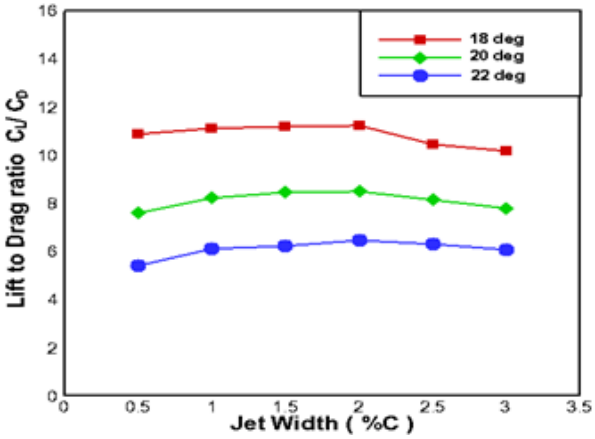

Figure 6. Evolution of lift to drag ratio on NACA0012 profile, M=0.13 for different values of jet width and angle of attack $\alpha = 18^0, 20^0, 22^0$

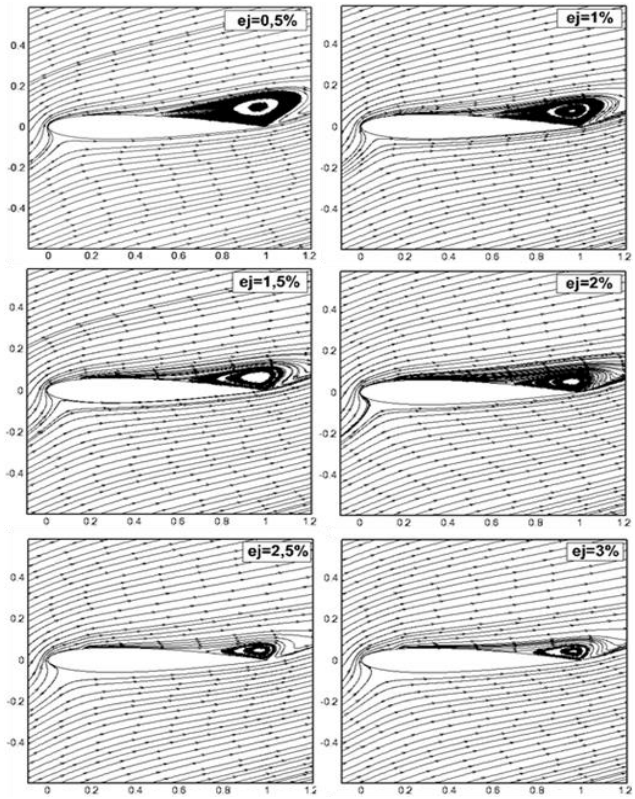

Figure 7. Streamlines pattern in flow field for on NACA0012 profile, M=0.13 for different values of jet width and angle of attack $\alpha=20^0$

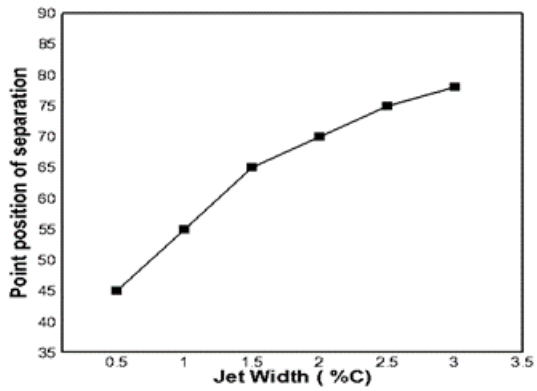

Figure 8. Evolution of point position of separation on NACA0012 profile, M=0.13 and $\alpha = 20^0$ for different values of jet width

4.2 Effect of momentum coefficient on the separation control

In this part, the numerical simulations will concentrate on the study of the effect of momentum coefficient and jet slope angle $\beta=45^0$ with width jet 2% of the chord length, located at 15%c from the leading edge of the airfoil. When the results were compared with without control flow. Figures 9, 10 present the lift and drag coefficients for different angles of attack for momentum coefficients values 0.045, 0.101, 0.18. From figure 9, one can see when the momentum coefficient is increased up to 0.045. The flow control does bring a slightly larger effect at low angle of attack (until $\alpha=10^0$). Where the flow is mainly attached to the airfoil body. For the higher angles of attack, when the separation is more obvious and affects more the flow patterns. The control enhances the lift

coefficient significantly by energizing the boundary layer and therefore delaying the separation. Under the present jet parameter, the lift is increased by 24.82%, 54.50%, 85.93%, and stall angle of attack is delayed by 2^0 (from 16^0 to 18^0), 4^0 (from 16^0 to 20^0), 6^0 (from 16^0 to 22^0), respectively, compared with an uncontrolled (without control) case. Where an improvement of stall angle obtained in this study. Whereas, in figure 10, we can see, when the momentum coefficient is increased up to 0.18, almost a no improvement is obtained of the drag coefficient for angles of attack lower than 10^0. Beyond this angle of attack, the drag coefficient increase for momentum coefficients 0.045, 0.101, 0.18 compared with uncontrolled case. Where the synthetic jet makes the boundary layer more turbulent. It, therefore, provides a higher level of drag with a lift gain. The flow control leads to an additive drag clearly noticed for the controlled airfoil in this range of angles of attack.

Figure 11 shows the averaged flow fields in one period for angle of attack $\alpha=24^0$ and jet slope angle $\beta=45^0$, the detail of the flow field is illustrated by streamline pattern. Three flow fields controlled by different jet momentum coefficient with the values $C\mu$= 0.045, 0.101 and 0.18, respectively, were compared with an uncontrolled case (without control). We can see that the separation zone is reduced. Where the separation is almost eliminated at $C\mu$=0.18 case. Indicating an improvement in aerodynamic performance.

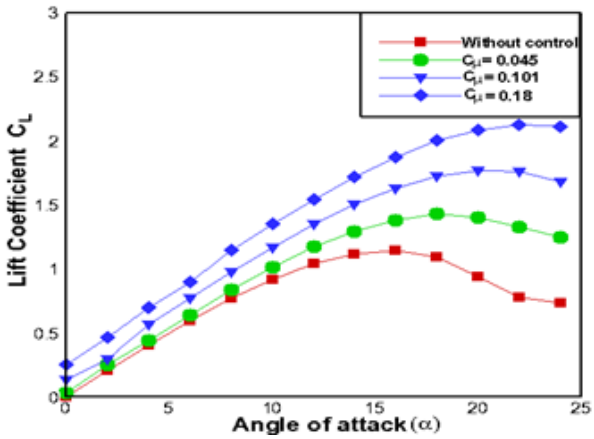

Figure 9. Effect of momentum coefficient with jet slope $\beta=45^0$ on lift coefficient over NACA0012 profile, M=0.13 with and without control for versus angle of attack

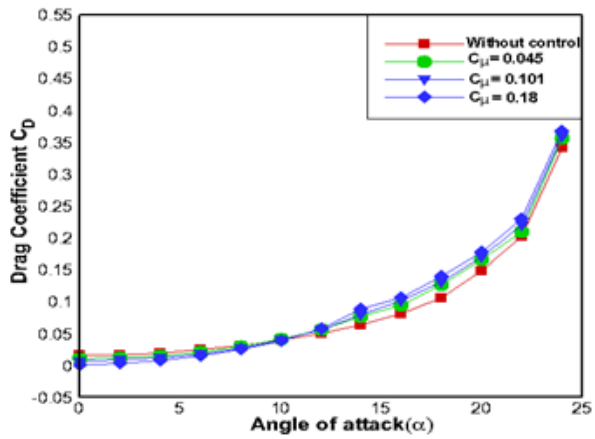

Figure 10. Effect of momentum coefficient with jet slope $\beta=45^0$ on drag coefficient over NACA0012 profile, M=0.13 with and without control for versus angle of attack

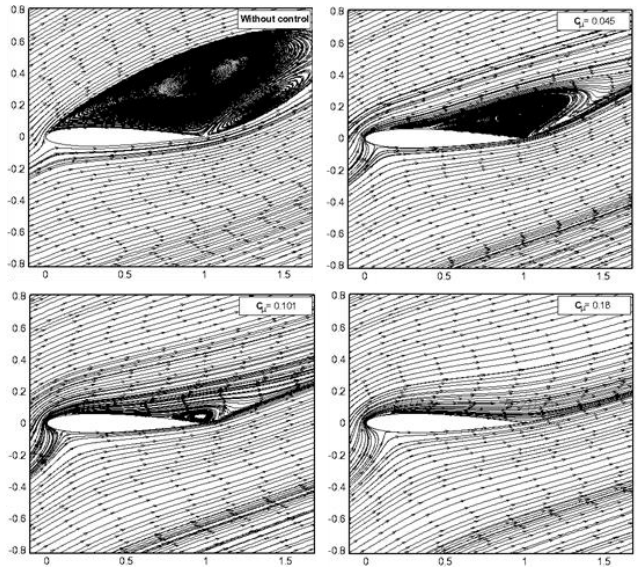

Figure 11. Streamlines pattern in flow field for on NACA0012 profile, M=0.13 for different values of momentum coefficient and angle of attack $\alpha=24^0$ and jet slope angle $\beta=45^0$

The lift, obtained from the flow control with perpendicular synthetic jet ($\beta= 90^0$) for different angles of attack, is shown in Figure 12. The aerodynamic performances were compared with an uncontrolled case (without control). This comparison shows that the perpendicular synthetic jet is still no apparent improvement in lift with the increase of jet momentum coefficient up to 0.18, the maximum lift is even decreased and stall angle of attack not delayed. In these cases, the momentum of the jet added to the boundary layer mixture generates a larger vortex structure.

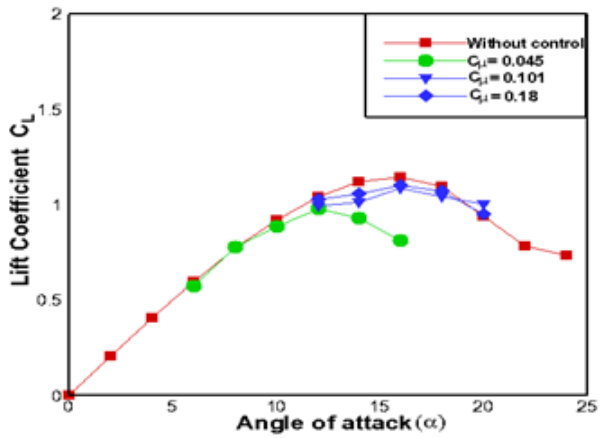

Figure 12. Effect of momentum coefficient with jet slope $\beta=90^0$ on lift coefficient over NACA0012 profile, M=0.13with and without control for versus angle of attack

The following figures 13 show the averaged flow fields in one period under the angle of attack $\alpha=16^0$ and jet slope angle $\beta=90^0$ conditions. The detail of the flow field is illustrated by streamline pattern. The momentum coefficient adversely affects the flow characteristics. We can see that perpendicular jet at different jet momentum coefficient creates a larger bubble separation for 0.045 cases and bubble separation with reattachment for 0.101, 0.18 cases, respectively compared with an uncontrolled case (without control). Which is synonymous with performance degradation.

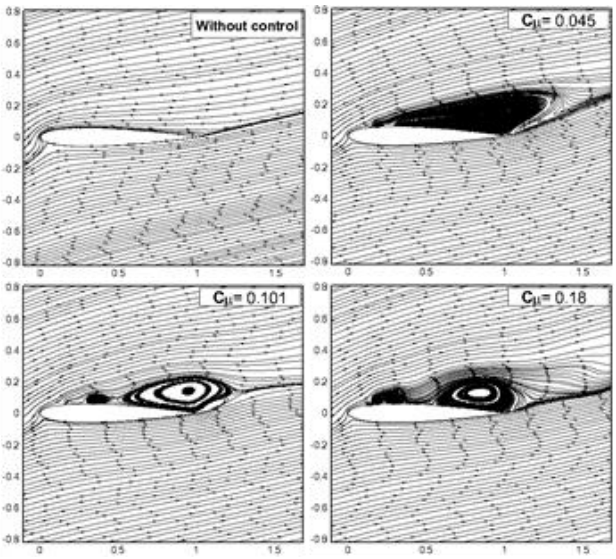

Figure 13. Streamlines pattern in flow field for on NACA0012 profile, M=0.13 for different values of momentum coefficient and angle of attack $\alpha=16^0$ and jet slope angle $\beta=90^0$

5. CONCLUSIONS

In this study, the effects of three parameters such as the width jet and jet momentum coefficients for different angles of attack on NACA0012 airfoil are examined and analyzed to flow separation control. The results suggest two key to improve aerodynamic performance. First, with jet slope angle $\beta=45^0$ by increasing jet width lift to ratio increase indicated best value in jet width equal to 2% of chord length where the bubble separation is shifted until to 70% of chord near the trailing edge for angle of attack $\alpha=20^0$. Second, another key can be used such as momentum coefficient with jet slope angle $\beta=45^0$ for different angles of attack. Where the stall angle is delayed up to 6^0 by increasing the jet momentum coefficient from 0.045 to 0.18 caused an acceleration of flow, Where the separation is almost eliminated in $C\mu=0.18$ case. Whereas, for jet slope angle $\beta=90^0$ by increasing momentum coefficient does not indicate any improvement in performance.

REFERENCES

[1] Wygnanski IJ. (1997). Boundary layer and flow control by periodic addition of momentum. AIAA 97-2117.

[2] Greenblatt D, Wygnanski IJ. (2000). Control of flow separation by periodic excitation. Progress in Aerospace Sciences 36(7): 487-545. https://doi.org/10.1016/S0376-0421(00)00008-7

[3] Corke T. (2002). Design of aircraft, Prentice-Hall, New York.

[4] Gillero P. (2011). Analytical models for the limiting condition of a pulsed jet control. 20th French Congress of Mechanics, Besançon, August 29th to September 2nd, 2011.

[5] Modi VJ, Hill SS, Yokomizo T. (1995). Drag reduction of trucks through boundary-layer control. Journal of Wind Engineering and Industrial Aerodynamics 54(3): 583-594. https://doi.org/10.1016/0167-6105(94)00074-n

[6] Jirasek A. (2004). A vortex generator model and its application to flow control. AIAA 2004-4965.

[7] Wygnanski IJ. (2004). The variables affecting the control of separation by periodic excitation. AIAA 2004-2505.

[8] Yousefi K Saleh R. (2014). The effects of trailing edge blowing on aerodynamic characteristics of the NACA0012 airfoil and optimization of the blowing slot geometry. Journal of Theoretical and Applied Mechanics 52(1): 165-179.

[9] Collins FC. (1979). Boundary layer control on wings using sound and leading edge serration. AIAA 1979-1875.

[10] Chang PK. (1976). Control of flow separation, hemisphere. Washington, DC.

[11] Gad-el-Hak M. (2000). Flow control, passive, active and reactive management. Cambridge Univ. Press, Cambridge, UK.

[12] Tuck A, Soria AJ. (2004). Active flow control over NACA 0015 airfoil using ZNMF jet. 15th Australasian Fluid Mechanics Conference.

[13] Zaman KBMQ, Bar-Sever A, Mangalam SM. (1987). Effect of acoustic excitation on the flow over a low-Re airfoil. Journal of Fluid Mechanics 182(1): 127-148. https://doi.org/10.1017/s0022112087002271

[14] Tang H, Salunkhe P, Zheng YY, Du JX, Wu YH. (2004). On the use of synthetic jet actuator arrays for active flow separation control. Experimental Thermal and Fluid Science 57(2004): 1-10.

[15] McCormick DC. (2000). Boundary layer separation control with directed synthetic jets. AIAA 2000-0519.

[16] Rizzeta DP, Visbal MR, Stank MJ. (1999). Numerical investigation of synthetic jet flow fields. AIAA Journal 37: 919-927.

[17] Wu JZ, Lu XY, Denny AG, Fan M, Wu JM. (1998). Post-Stall flow control on an airfoil by local unsteady forcing. Journal of fluid Mechanics 371: 21-58.

[18] Nae C. (1998). Synthetics jets influence on NACA0012 airfoil at high angle of attacks. AIAA papers 98.

[19] Rosas CR. (2005). Numerical simulation of flow separation control by oscillator fluid injection. Doctor of Philosophy Thesis, A&M University, Texas.

[20] Esmaeili H, Tadjfar M, Bakhtian A. (2014). Tangential synthetic jets for separation control. Journal of fluids and structures 45: 50-65.

[21] Donovan JF, Kral LD, Cary AW. (1998). Active flow control applied to an airfoil. AIAA Paper 98-0210.

[22] Piperas AT. (2010). Investigation of boundary layer suction on a wind turbine airfoil using CFD. Master thesis. Technical University of Denmark.

[23] You D, Moin P. (2008). Active control of flow separation over an airfoil using synthetic. Journal of Fluids and Structures 24: 1349-1357.

[24] Akcayoz E Tuncer IH. (2009). Numerical investigation of flow control over an airfoil using synthetic jets and its optimization. International Aerospace Conference, Turkey.

[25] Montazer E, Mirzaei M, Salami E, Ward TA, Romli FI, Kazi SN. (2016). Optimization of a synthetic jet actuator for flow control around an airfoil. IOP Conference series: Materials Science and Engineering 152(2016): 012023. https://doi.org/10.1088/1757-899X/1/012007

[26] Boukenkoul MA, Li FC, Aounallah M. (2017). A 2D simulation of the flow separation control over a NACA0015 airfoil using a synthetic jet actuator. IOP Conference Series: Materials Science and Engineering

187(2017): 012007. https://doi.org/10.1088/1757-899x/1/012007
[27] Abed KN, Azzawi IDJ. (2015). Control of flow separation over NACA0015 airfoil using synthetic jet actuators. Diyala Journal of Engineering Sciences 674-685.
[28] Crook A, Wood NJ. (2001). Measurements and Visualizations of synthetic jets. AIAA Paper 2001-0145.
[29] Glezer, Amitay M. (2002). Synthetic Jets. Annu. Rev. Fluid Mech 34: 503-529.
[30] Smith BL, Glezer A. (1997). Victoring and small-scalemotions effected in free shear flows using synthetic jet actuators. AIAA 35th Aerosp. Sci. Meet 97-0213.
[31] Smith BL, Glezer A. (1999). Victoring of a high ratio rectangular air jet using a zero net-mass- flux control jet. Bul, Am Phys Soc 39: 1894.
[32] Yousefi MK, Salah R. (2014). The effect of trailing edge blowing on aerodynamic characteristics of the NACA0012 airfoil and optimization of the blowing slot geometry. Journal of Theoretical and Applied Mechanics Warsaw 165-179.
[33] Gregory N, Reilly CLO. (1973). Low-speed Aerodynamic Characteristics of NACA0012 Aerofoil section, including the effects of upper-surface roughness simulating hoar frost. Aerodynamics division N.P.L. Aeronautical Research Council. London.
[34] Luo DH, Sun XJ, Huang DG, Wu GQ. (2011). Flow control effectiveness of synthetic jet. Stalled Airfoil March 225 Part C: 2106-2114. https://doi.org/10.1177/0954406211407255

NOMENCLATURE

C_f	skin friction coefficient
C_P	pressure coefficient
C_D	drag coefficient
C_L	lift coefficient
$C\mu$	jet momentum coefficient
c	chord length
F^+	non dimentionnal jet frequency
f	jet frequency
e_j	relative jet width
Re	Reynolds number
U_0	jet velocity amplitude
U_j	jet velocity
U	upstream velocity
M	Mach Number
V_r	relative velocity

Greek symbols

α	angle of attack
β	angle between jet velocity and chord
ρ_j	jet density
ρ	freestream density

Subscripts

f	friction
D	Drag
L	Lift
P	Pressure
r	relative
j	jet
μ	momentum